Int J Adv Manuf Technol (2017) 93:2155–2160
DOI 10.1007/s00170-017-0630-5

ORIGINAL ARTICLE

FEA of vertical parts formed with multistage incremental sheet metal forming based on the forming limit stress diagram

Mengling Wu[1,2,3] · **Guangcheng Zha**[2,3] · **Gan Zirui**[2,3]

Received: 23 January 2017 / Accepted: 5 June 2017 / Published online: 27 June 2017

Abstract Multistage incremental sheet metal forming (MS-ISF) is used to produce sheet metal parts with a large forming angle. Similar to the forming limit diagram (FLD) in stamping, FLD in MS-ISF is not sufficiently reliable due to the effect of loading path. To solve this problem, a method to calculate the forming limit stress diagram (FLSD) from FLD was proposed. Experiments proved that FLSD is a reliable fracture indicator that is unaffected by the loading path in MS-ISF.

Keywords Multistage incremental forming · Formability · Loading path · Forming limit stress diagram

1 Introduction

Incremental sheet metal forming (ISF) is a cheap and fast method of producing sheet metal parts in small batches [1–3]. A tool with a hemispherical end moves along a series of counters to deform the sheet metal blank layer by layer. The maximum deformation in ISF is extremely high due to localized deformation [4, 5]. In current studies on ISF formability, most achievements focus on single-stage ISF (SS-ISF) [6–8]. The maximum forming angle θ_{max} and forming limit diagram (FLD) are two indicators of SS-ISF formability [6]. For most SS-ISF parts, the deformed sheet is in the plane strain state. The major and minor strains can be described as

$$\begin{cases} \varepsilon_1 = \ln\left(\dfrac{1}{\cos\theta}\right), \\ \varepsilon_2 = \quad 0 \end{cases} \tag{1}$$

where θ is the forming angle. For special cases, such as those using large tools to form small parts, minor strain ε_2 is not equal zero. For these parts, the maximum forming angle θ_{max} cannot indicate deformation at the fracture point, and only FLD can represent formability.

Filice used six different materials to test the formability in SS-ISF and obtained FLD by forming the conical parts of a constant forming angle [6]. Hussain proposed two methods, namely, varying wall angle conical frustum test and varying wall angle pyramid frustum test, to obtain FLD. Both methods reduced the steps for testing the formability of SS-ISF [7, 8].

Multistage ISF (MS-ISF) was proposed to produce parts with a large forming angle [9]. Compared to SS-ISF, deformation in MS-ISF is significantly more complex, and minor strain ε_2 is not equal zero [9, 10]. Thus, the maximum forming angle θ_{max} cannot be an indicator in MS-ISF. To solve the problem, Shi suggested a method to test formability (FLD) in MS-ISF by forming vertical parts with different stages; however, the test results showed that the forming limit was affected by forming stage parameters (i.e., three forming limit curves (FLCs) were gained from test results for the same material) [11]. Such outcome reveals that FLD cannot be employed as a reliable criterion for MS-ISF. Thus, proposing a criterion that is unaffected by the forming stage parameters is important and meaningful for MS-ISF.

FLD should be accurately named as forming limit strain diagram. Moreover, the FLD that utilizes the major and minor strains at the fracture points could be used to judge the

✉ Mengling Wu
wmlzl@njit.edu.cn

[1] College of Mechanical and Electrical Engineering, Nanjing University of Aeronautics and Astronautics, Nanjing 210016, China

[2] School of Materials Science and Engineering, Nanjing Institute of Technology, Nanjing 211167, China

[3] Jiangsu Key Laboratory of Advanced Structural Materials and Application Technology, Nanjing 211167, China

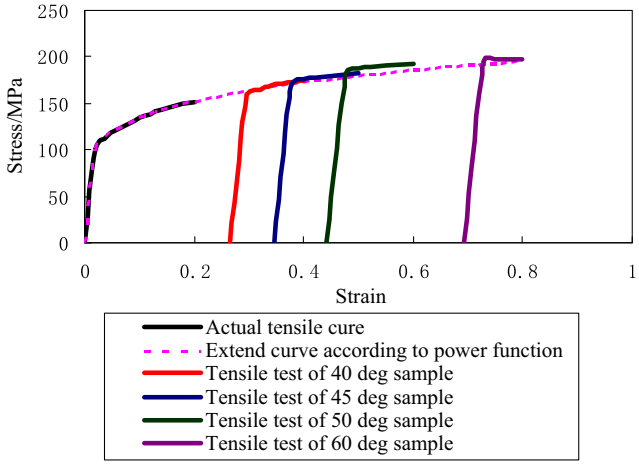

Fig. 1 Tensile test result

possibility of crack. The problem for FLD is that the loading path (i.e., the variation in the strain during the forming process) affects the final test result [12, 13]. To solve this problem, researchers proposed the FLSD and confirmed it as a reliable criterion for stamping [14]. Similar to stamping, FLD in MS-ISF was proven as a loading path-related criterion [11].

To identify a reliable crack criterion, researchers recommended the forming limit stress diagram (FLSD) and discovered that the loading path does not affect FLSD [15, 16]. Thus, suggesting that FLSD can be employed in MS-ISF is considerably logical.

2 Material property test

Material elongation in ISF is remarkably larger than that in tensile test, and the property of deformed material should first be studied. AA1060-O sheet with a thickness of 0.9 mm was employed for all tests. Pyramid parts of four types with forming angles of 40°, 45°, 50°, and 60° were formed by SS-ISF (i.e., equivalent strain is 0.266, 0.346, 0.442, and 0.693, respectively). Then, tensile tests were conducted with samples cut from the deformed area. Results show that although deformation in ISF is larger than that in tensile

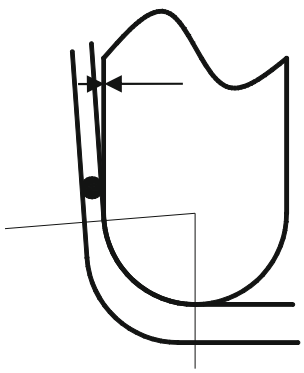

Fig. 2 Location of fracture point

Table 1 Changes in material property before and after ISF

	Rolling direction before ISF	Vertical direction before ISF	Rolling direction after ISF	Vertical direction after ISF
Yield stress (MPa)	110.6	108.2	193.2	180.3

Fig. 3 ISF machine developed by NUAA

deformation, the property of the deformed material still obeys the power law (Fig. 1).

3 Method of obtaining FLSD

FLSD is gained from FLD according to the relation between stress and strain [14, 16]. Mohr's circle of stress and strain is a

Table 2 Forming strategy and processing parameters

Test	Forming strategy (°)	Tool diameter (mm)	Step size (mm)	Top diameter (mm)
1	20–90	10	0.5	110
2	30–90			
3	40–90			
4	50–90			
5	60–90			
6	20–60–90			
7	30–70–90			
8	40–60–90			
9	40–70–90			
10	50–70–90			
11	50–60–70–90			

Fig. 4 Parts for formability test of MS-ISF

pair of similar shape. In ISF (both SS-ISF and MS-ISF), fracture occurs in the area where the tool and the blank have no contact with each other (Fig. 2). Hence, the third principle stress can be defined as zero.

$$\sigma_3 = 0. \tag{2}$$

Tensile tests were performed to compare the difference in material property caused by ISF. Pyramid parts of 60° forming angle were formed, and tensile samples were cut in the rolling and vertical directions (Table 1). Test results show that yield stress increases by work hardening; however, the difference in rolling and vertical directions is not significant.

Suppose that the material is continuous and isotropic in the plane of the blank, α is defined as

$$(\sigma_1\text{-}\sigma_2)\Big/(\sigma_2\text{-}\sigma_3) = (\varepsilon_1\text{-}\varepsilon_2)\Big/(\varepsilon_1\text{-}\varepsilon_3) = \alpha. \tag{3}$$

Thus, the equivalent stress $\overline{\sigma}$ is

$$\begin{aligned}\overline{\sigma} &= \frac{1}{\sqrt{2}}\sqrt{(\sigma_1\text{-}\sigma_2)^2 + (\sigma_2\text{-}\sigma_3)^2 + (\sigma_3\text{-}\sigma_1)^2} \\ &= \frac{1}{\sqrt{2}}\sqrt{(\sigma_1\text{-}\sigma_2)^2 + \sigma_2^2 + \sigma_1^2} = \sqrt{\frac{1+\alpha^2}{2}}\sigma_2.\end{aligned} \tag{4}$$

According to Eqs. 3 and 4, major and minor stresses can be defined as

$$\begin{cases}\sigma_2 = \sqrt{\dfrac{2}{1+\alpha^2}}\overline{\sigma}. \\ \sigma_1 = (1+\alpha)\sigma_2\end{cases} \tag{5}$$

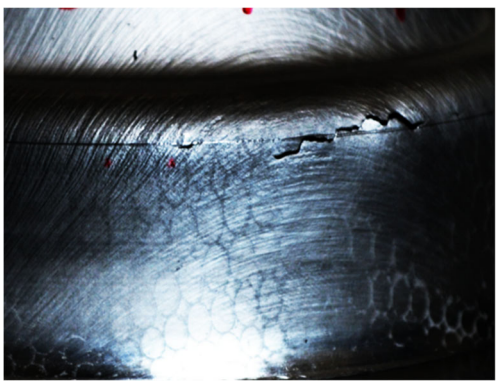

Fig. 5 Grids near the fracture point

As indicated in Fig. 2, the property of deformed material obeys the power law, and $\overline{\sigma}$ in Eq. 5 can be obtained from the tensile test for the unformed blank. After obtaining the hardening index K and the hardening coefficient n, $\overline{\sigma}$ can be defined as follows:

$$\overline{\sigma} = K\overline{\varepsilon}^{\,n}, \tag{6}$$

where

$$\overline{\varepsilon} = \frac{\sqrt{2}}{3}\sqrt{(\varepsilon_1\text{-}\varepsilon_2)^2 + (\varepsilon_2\text{-}\varepsilon_3)^2 + (\varepsilon_3\text{-}\varepsilon_1)^2}. \tag{7}$$

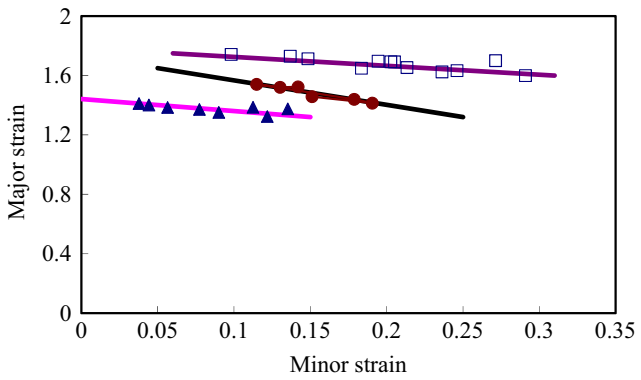

Fig. 6 FLD of both single-stage ISF and MS-ISF

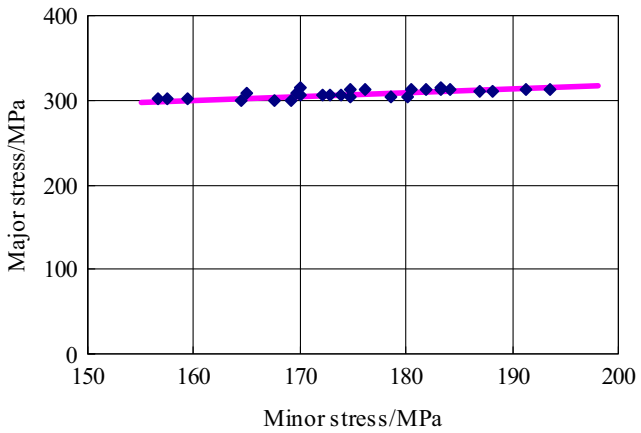

Fig. 7 FLSD results

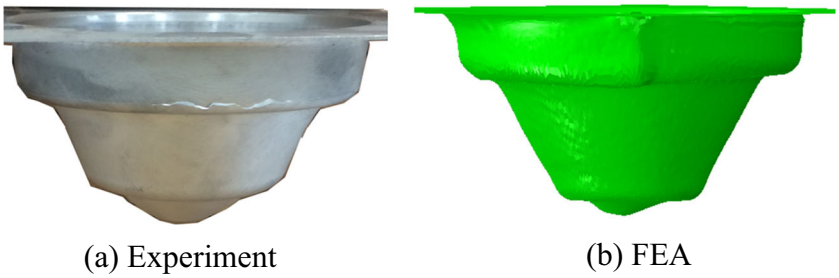

Fig. 8 Parts gained from experiment and FEA. **a** Experiment. **b** FEA

4 Experiments

To study the differences between FLD and FLSD, all parameters and test method are the same as those in [11].

4.1 Materials and setup

Aluminum alloy AA1060-O sheet of 0.9-mm thickness was employed. A professional ISF machine developed by the Nanjing University of Aeronautics and Astronautics was used to perform the test (Fig. 3).

4.2 Forming strategy and processing parameters

Forming strategy and processing parameters are shown in Table 2. In all tests, the model used in the last stage is a part with a vertical wall, and the forming operation was ended as soon as fracture occurred.

5 Experimental results and discussion

5.1 FLD of MS-ISF

Figure 4 shows the parts used in the test, whereas Fig. 5 shows the deformed grids after forming. After all parts were formed, the deformation of grids at fracture points was measured. Major and minor strains (ε_1 and ε_2) can be calculated as follows:

$$\begin{cases} \varepsilon_1 = \ln\left(d_1 / d_0\right) \\ \varepsilon_2 = \ln\left(d_2 / d_0\right) \end{cases}, \tag{8}$$

where d_1 and d_2 are the dimensions of the long and short axes of the deformed grid, respectively, and d_0 is the initial diameter of grids.

Figure 6 shows the FLD results of the test, where three FLCs are clearly present [12]. An important application for FLD is used as the fracture criteria in finite element analysis (FEA). The FLD shown in Fig. 6 contains three FLCs. Determining the optimal choice is difficult for an FEA operator; thus, FLD cannot be considered as a good fracture criterion in MS-ISF.

5.2 FLSD results

Major and minor stresses were calculated using Eqs. 2–7 (K = 203 MPa, n = 0.18). Figure 7 shows the FLSD results of MS-ISF. Compared with the FLD result shown in Fig. 6, the FLSD results in Fig. 7 are remarkably more reliable and are unaffected by the loading path. Such outcome indicates

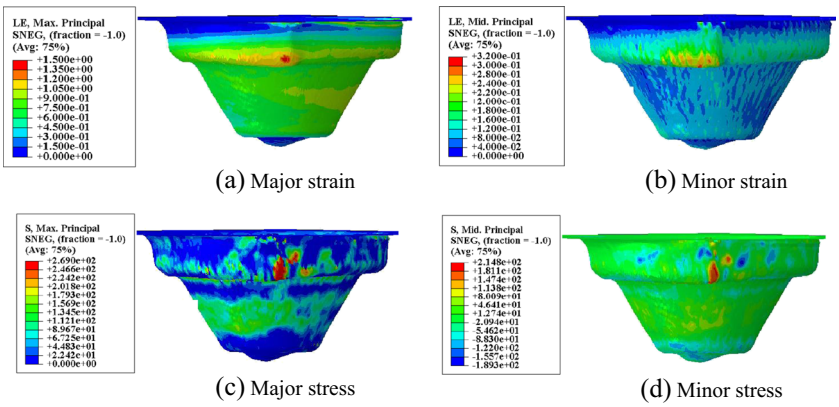

Fig. 9 FEA results. **a** Major strain. **b** Minor strain. **c** Major stress. **d** Minor stress

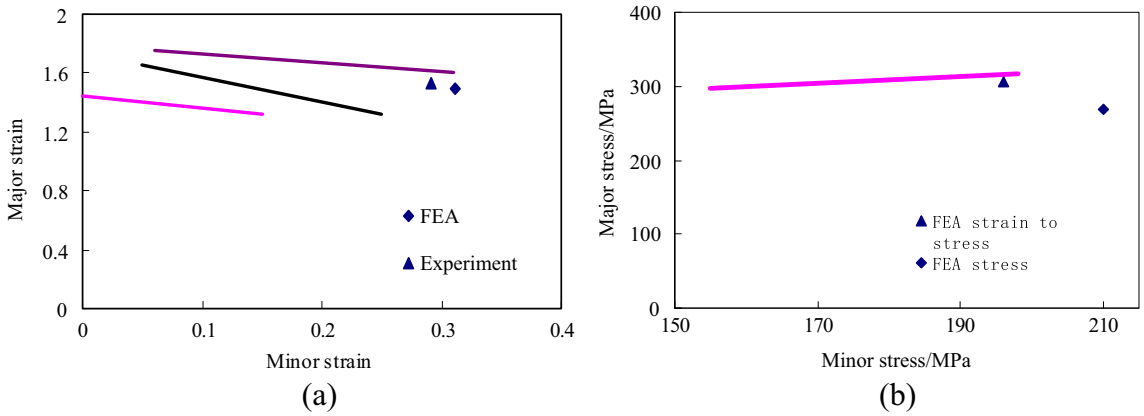

Fig. 10 FEA results in fracture point shown in **a** FLD and **b** FLSD

that FLSD can be employed as a fracture criterion with high accuracy not only for stamping but also for MS-ISF.

6 FEA test

A dynamic code was programmed to simulate the forming process to prove the application of FLSD in the FEA of MS-ISF. Shell elements with 0.8-mm average size were employed to construct the blank. In the FEA model, material property and processing parameters (except forming speed) are all similar to those used in the experiments. Forming speed was set as 20 m/s to save calculation cost. The model used in FEA is a part formed with 30°–60°–90° forming strategy. An experiment was also conducted to prove the accuracy of FEA. Figure 8 shows the final shape of parts obtained by the experiments and FEA.

The forming depth of the last stage in FEA was set as 24.8 mm, which is equal to the fracture depth in the experiment. Figure 9 shows the FEA results of the major and minor strains and major and minor stresses. The maximum values of these four parameters are located in the area where the blank is in contact with the tool.

The maximum values of the major and minor strains obtained from FEA are 1.492 and 0.312, respectively, whereas those obtained from the experiment are 1.531 and 0.291, respectively. Although the FEA results in strain are remarkably similar to the experimental results, the strain is located in the area between the second and the third FLCs. Deciding which FLC should be employed is challenging (Fig. 10a). The maximum values of the major and minor stresses are 269 and 210 MPa, respectively, and are located below the forming limit stress curve (FLSC) (Fig. 10b). However, in the experiments, fracture occurs in this area.

The dynamic method performs poorly in stress calculation. The strain result of FEA is accurate; thus, it can be used to calculate stress distribution. Based on strain gained from FEA and Eqs. 2–7, the major and minor stresses can be considered as 305 and 196 MPa, respectively; these values are only slightly lower than those of the FLSC (Fig. 10b). With this method, the FLSD of MS-ISF can be employed in the FEA for the same material. During the calculation, stress can be obtained

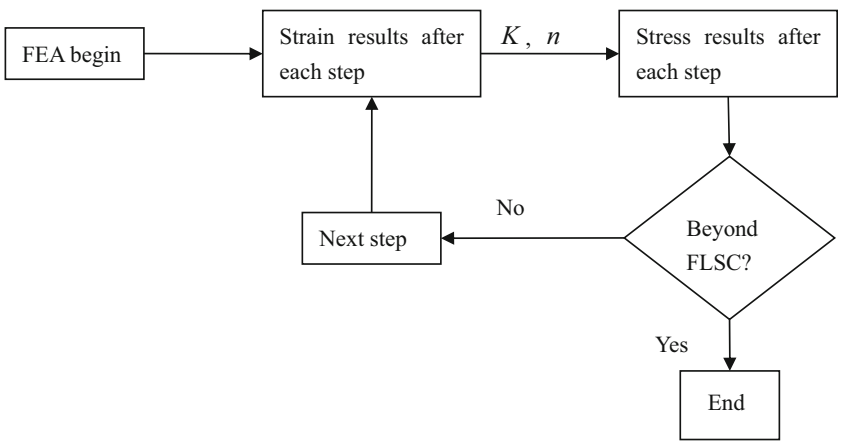

Fig. 11 Application of FLSD in FEA

Table 3 Depth of fracture points obtained by experiments and FEA

Material	Forming strategy (°)	Depth of fracture points gained by experiments (mm)	Depth of fracture points obtained by FEA (mm)
AA3003-O	45–90	15.6	16.7
	45–65–90	21.3	22.4
	55–65–75–90	25.8	24.3
AA2024-O	45–90	13.2	14.4
	45–65–90	19.6	18.9
	55–65–75–90	26.7	26.4
DC04	45–90	17.5	18.3
	45–65–90	23.2	24.6
	55–65–75–90	28.7	29.4

based on the strain distribution after each step. Before starting the next step, a stress judgment should be performed. Only when the stress distribution is lower than FLSC should the calculation be continued (Fig. 11).

Three additional materials (i.e., AA3003-O, AA2024-O, and DC04) were employed in performing the MS-ISF formability test to prove the reliability of the study. According to the proposed method, FLSD was obtained. FEA calculation was terminated based on the method shown in Fig. 11. Table 3 shows the depth of fracture points obtained by the experiments and FEA. Evidently, FEA results based on FLSD criterion are sufficiently accurate.

7 Conclusions

The main conclusions in this study are as follows:

1. In the formability test of MS-ISF, FLC is affected by the forming strategy.
2. Using FLD to calculate FLSD is feasible for the formability test of MS-ISF.
3. Similar to the formability test of stamping, FLSD is unaffected by the loading path and can be employed as a reliable criterion in MS-ISF.
4. The FLSD of MS-ISF can be employed as a crack criterion in FEA.

Acknowledgements This research is supported by the Scientific Foundation of Nanjing Institute of Technology (Project No. CKJB201402)

References

1. Park JJ, Kim YH (2003) Fundamental studies on the incremental sheet metal forming technique. J Mater Proc Tech. 140:447–453
2. Kitazawa K, Okaku H (1996) Possibility of CNC incremental stretch-expanding of sheet metal by single-tool-path process. Trans Japan Sci Mech Eng 62(597):2012–2017
3. Jeswiet J, Micari F, Hirt G, Bramley A, Duflou JR, Allwood JM (2005) Asymmetric single point incremental forming of sheet metal. Ann CIRP 54(2):623–650
4. Amino H, Lu H, Ozawa S, Fukuda K, Maki T (2002) Dieless NC forming of automotive service panels. Proc Conf Adv Tech Plasticity:1015–1020
5. Ambrogio G, De Napoli L, Filice L, Gagliardi F, Muzzupappa M (2005) Application of incremental forming process for highly customized medical product manufacturing. J Mater Proc Tech 162-163:156–162
6. Fratini L, Ambrogio G, Lorenzo RD (2004) Influence of mechanical properties of the sheet material on formability in single point incremental forming. Ann CIRP 2004(53):207–210
7. Hussain G, Gao L (2007) A novel method to test the thinning limits of sheet metals in negative incremental forming. Int J Mach Tools Manuf 47:419–425
8. Hussain G, Lin G (2007) An experimental study on some formability testing method in incremental forming. J Mater Proc Tech 186: 45–53
9. Dongkai X, Rajiv M, Venkata R (2012) Analytical prediction of stepped feature generation in multi-pass single point incremental forming. J Manuf Pro 14:487–494
10. Duflou JR, Verbert J, Belkassem B, Gu J, Sol H, Henrard C, Habraken AM (2008) Process window enhancement for single point incremental forming through multi-step toolpaths. Ann CIRP 57:253–256
11. Shi X, Hussain G, Zha G, Wu M, Kong F (2014) Study on formability of vertical parts formed by multi-stage of incremental forming. Int J Manuf Technol 75(4):1049–1053
12. Kohara S (1993) Forming limit curves of aluminum and aluminum alloy sheets and effects of strain path on the curves. J Mater Process Tech 38:723–735
13. Chow CL, Yu LG, Tai WH, Demeri MY (2001) Prediction of forming limit diagrams for AA6111-T4 under non-proportional loading. Inter J Mech Sci 43:471–486
14. Arrieux R (1997) Determination and use of the forming limit stress surface of orthotropic sheets. J Mater Proc Tech 54:25–32
15. Haddad A, Vacher P, Arrieux R (1999) Numerical determination of forming limit diagrams of orthotropic sheets using the '3G' theory of plasticity. J Mater Pro Techn 42(43):419–423
16. Sing W, Rao K (1997) Study of sheet metal failure mechanisms based on stress-state conditions. J Mater Proc Techn 67:201–206